NOTES AND CORRESPONDENCE

Comments on "Critical Test of the Validity of Monin–Obukhov Similarity during Convective Conditions"

EDGAR L ANDREAS

U. S. Army Cold Regions Research and Engineering Laboratory, Hanover, New Hampshire

BRUCE B. HICKS

NOAA/Air Resources Laboratory, Silver Spring, Maryland

12 July 2001 and 21 December 2001

1. Our concern

An inherent problem in validating Monin–Obukhov similarity theory is that, often, there are simply not enough independent scaling variables. As a result, a scale used to nondimensionalize the dependent variable sometimes appears in the nondimensionalization for the independent variable. Plots of these nondimensional variables can then display seemingly good or bad correlations that are really fictitious. In other words, these plots reflect the statistics of the common variables rather than something fundamental about atmospheric physics (Hicks 1978a,b, 1981, 1995; Kenney 1982). We worry that Johansson et al. (2001) may have based their main conclusions on such fictitious correlations rather than on real physics.

2. Scatter in plots of ϕ_m and ϕ_h

In conventional plots of nondimensional wind (ϕ_m) and temperature (ϕ_h) gradients against nondimensional height ($\zeta \equiv z/L$), as in Figs. 1, 2, 6, and 16 of Johansson et al. (2001), the friction velocity (u_*) appears in both axes. Remember,

$$\phi_m\left(\frac{z}{L}\right) = \frac{kz}{u_*}\frac{\partial U}{\partial z}, \tag{1}$$

$$\phi_h\left(\frac{z}{L}\right) = \frac{kzu_*}{\overline{w't'}}\frac{\partial \Theta}{\partial z}. \tag{2}$$

Here, z is the measurement height; k, the von Kármán constant; $\overline{w't'}(\equiv Q_0)$, the $w' - t'$ covariance in the atmospheric surface layer; and $\partial U/\partial z$ and $\partial\Theta/\partial z$, the near-surface vertical gradients in wind speed and potential temperature. Following Johansson et al. (2001), we include moisture effects in the Obukhov length L and thus define it as

$$L = -\frac{u_*^3 T_0}{kgQ_0\left(1 + \dfrac{0.07}{\beta}\right)}, \tag{3}$$

where g is the acceleration of gravity, T_0 is the average absolute temperature in the surface layer, and β is the Bowen ratio.

Consider the consequences if all terms on the right-hand sides of (1) and (2) were measured accurately except u_*, which is typically measured with no better than $\pm 10\%$ accuracy. Denote this measured u_* value as

$$u_{*M} = u_{*T} + \Delta u_*, \tag{4}$$

where u_{*T} is the true value and Δu_* is the measurement error. We can also write (4) as

$$u_{*M} = u_{*T}(1 + \delta u_*), \tag{5}$$

where $\delta u_* = \Delta u_*/u_{*T}$ is the uncertainty in the u_* measurement.

Substituting (5) into (1), (2), and (3) yields

$$\phi_{m,M} = \frac{\phi_{m,T}}{1 + \delta u_*}, \tag{6}$$

$$\phi_{h,M} = (1 + \delta u_*)\phi_{h,T}, \tag{7}$$

$$\zeta_M = \frac{\zeta_T}{(1 + \delta u_*)^3}, \tag{8}$$

where subscripts M and T denote "measured" and "true" values.

Corresponding author address: Dr. Edgar L Andreas, U. S. Army Cold Regions Research and Engineering Laboratory, 72 Lyme Road, Hanover, NH 03755-1290.
E-mail: eandreas@crrel.usace.army.mil

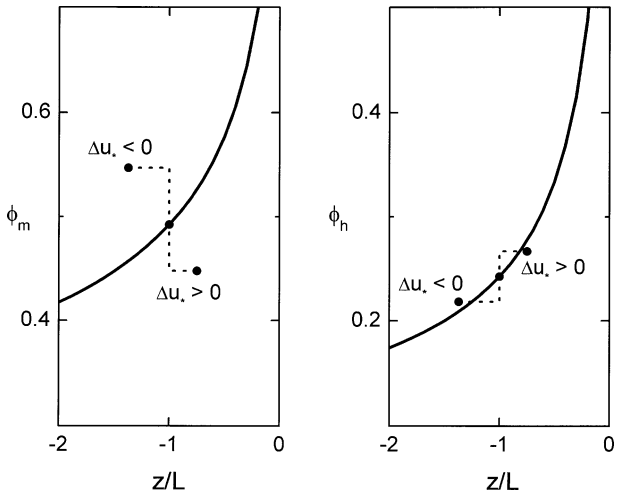

FIG. 1. The effects of ±10% errors in a measurement of u_* on plots of ϕ_m and ϕ_h in unstable stratification. Here the bold curves are assumed to be the true $\phi_m(\zeta)$ and $\phi_h(\zeta)$ functions. The markers on these lines are the true ϕ_m and ϕ_h values; that is, their coordinates are $(\zeta_T, \phi_{m,T})$ and $(\zeta_T, \phi_{h,T})$, respectively. The markers off the lines show measurements for which δu_* is −10% and +10%.

Equations (6)–(8) reveal that, for unstable stratification, an error in the u_* measurement tends to move a measured ζ–ϕ_m pair normal to the fitting curve (i.e., Figs. 1 and 6 in Johansson et al. 2001) and a measured ζ–ϕ_h pair along the fitting curve (i.e., Figs. 2 and 16 in Johansson et al.). For stable stratification, the opposite occurs: a ζ–ϕ_m pair moves along the fitting curve, while a ζ–ϕ_h pair moves normal to it. Figure 1 demonstrates these effects on plots of ϕ_m and ϕ_h when the u_* uncertainty (i.e., δu_*) is ±10% and the stratification is unstable.

Clearly, in unstable stratification, errors in u_* increase the apparent scatter in plots of ϕ_m but not in plots of ϕ_h. Likewise, (2) and (3) suggest that errors in measuring $\overline{w't'}$, another variable that ζ and ϕ_h share, tend to displace ζ–ϕ_h pairs along the fitting curve rather than normal to it. The repeated finding that, for unstable stratification, ϕ_m is more scattered than ϕ_h results, at least partially, because of the uncertainty in the common variable u_*. Thus, the ''striking difference in scatter'' between ϕ_m and ϕ_h plots that Johansson et al. (2001) use as the impetus to test for an additional scaling parameter—namely z_i, the height of the convective boundary layer—does not seem that compelling to us.

3. Nondimensionalizing horizontal velocity variance

We also worry that the paper by Johansson et al. (2001) may suffer from the effects of fictitious correlations in a deeper way. In their Figs. 9 and 12, for example, Johansson et al. (2001) plot the nondimensional horizontal velocity variance $(\sigma_h/w_*)^2$ versus the nondimensional length scale z_i/L. Here,

$$\sigma_h^2 = \frac{1}{2}(\overline{u'^2} + \overline{v'^2}) = \frac{1}{2}(\sigma_u^2 + \sigma_v^2), \tag{9}$$

where σ_u and σ_v are the standard deviations in the longitudinal and transverse components of the velocity vector. Also, according to definitions in Johansson et al. (2001), w_* is the convective velocity scale,

$$w_* = \left[\frac{g}{T_0}Q_0 z_i\left(1 + \frac{0.07}{\beta}\right)\right]^{1/3}. \tag{10}$$

From (3) and (10), we see that the independent variable that Johansson et al. (2001) use in their Figs. 9 and 12 is

$$\frac{z_i}{L} = -\frac{kgz_iQ_0}{T_0u_*^3}\left(1 + \frac{0.07}{\beta}\right) = -\frac{kw_*^3}{u_*^3}, \tag{11}$$

while, as we mentioned, their dependent variable is $(\sigma_h/w_*)^2$. That is, w_* appears prominently in both the dependent and independent variables.

In light of (11), even if we knew nothing about σ_h or u_*, we would speculate that $(\sigma_h/w_*)^2$ would be large when $-z_i/L$ is near zero (i.e., when w_* is small) and would be small when $-z_i/L$ is large (i.e., when w_* is large). This is just what Figs. 9 and 12 in Johansson et al. (2001) show. Johansson et al. interpret these plots as demonstrating that w_* is the appropriate scaling variable for σ_h over most of the z_i/L range; but clearly, the built-in correlation could weigh heavily in this conclusion.

The best way for Johansson et al. (2001) to see whether they have really found a useful relationship or have been misled by fictitious correlation is to randomize the w_* values in their dataset (e.g., Hicks 1978a, 1981), recompute $(\sigma_h/w_*)^2$, recompute z_i/L according to (11), and make another plot of $(\sigma_h/w_*)^2$ versus z_i/L. If the plot still looks like their Figs. 9 and 12, they have been victims of fictitious correlation. If, on the other hand, the new plot looks unpublishably confusing, they have indeed found a useful nondimensionalization.

Since we did not have access to the data that Johansson et al. (2001) used, we made the plot described above with totally random data. In an Excel spreadsheet, we created 100-point series of σ_h, u_*, and w_* values using a random number generator. We constrained the random values to plausible ranges: 0.3–2.0 m s^{-1} for σ_h, 0.05–0.70 m s^{-1} for u_*, and 0.5–2.6 m s^{-1} for w_*. From these values, we computed $(\sigma_h/w_*)^2$ and z_i/L from (11).

We further screened these $(\sigma_h/w_*)^2$ and z_i/L values to make sure they were ''realistic.'' That is, using Figs. 9 and 12 in Johansson et al. (2001) as guides, we discarded as outliers data lines for which $(\sigma_h/w_*)^2$ was outside the range 0.2–6, or for which z_i/L was outside the range −0.5 to −200. Eliminating these outliers reduced the original 100 lines of data to 56.

Figure 2 shows a plot of $(\sigma_h/w_*)^2$ versus z_i/L constructed from these random numbers. It is quite similar

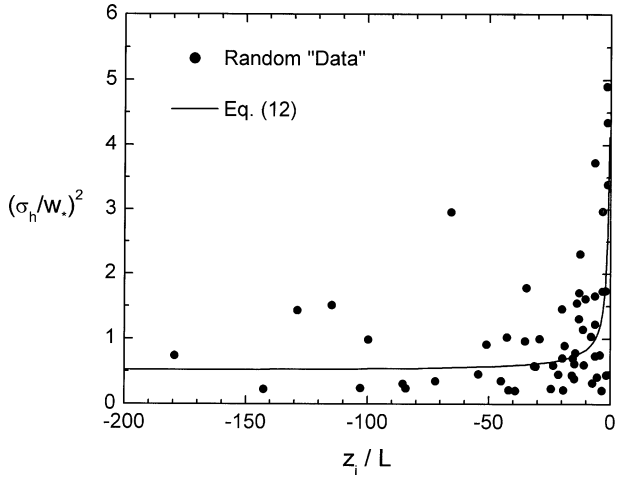

FIG. 2. An artifact of sharing variables in nondimensional plots. Here both σ_h and w_* are products of a random number generator. The nondimensional length scale z_i/L is also randomly produced from (11) using these same w_* values and randomly generated values of u_*. The line, our Eq. (12), is the fit suggested by Johansson et al. (2001).

to Figs. 9 and 12 in Johansson et al. (2001). Johansson et al. (2001) fit the data in their Figs. 9 and 12 with

$$\left(\frac{\sigma_h}{w_*}\right)^2 = k^{2/3}\left(\frac{10}{-z_i/L} + 0.88\right)^{2/3}. \tag{12}$$

Figure 2 shows this same line. Clearly this line represents the trend in the data markers well although the markers represent no physical process. The presence of w_* in both the vertical and horizontal axes simply makes such a plot a foregone conclusion.

Johansson et al. (2001) developed (12) following the suggestion by Panofsky et al. (1977) that

$$\left(\frac{\sigma_h}{u_*}\right)^2 = \left(12 - \frac{0.5z_i}{L}\right)^{2/3}. \tag{13}$$

Using (11), we rewrite (12) as

$$\sigma_h^2 = [10u_*^3 + 0.88kw_*^3]^{2/3}. \tag{14}$$

Likewise, we can rewrite (13) as

$$\sigma_h^2 = [12u_*^3 + 0.5kw_*^3]^{2/3}. \tag{15}$$

To us, either of these relations is much more transparent than the similarity relation that Johansson et al. (2001) suggest, (12). In (14) and (15), we clearly see what causes the variability in the horizontal wind components: shear-driven turbulence in high winds and convectively driven turbulence in low winds. Coincidentally, though different in mathematical detail, (14) has almost the same limiting values at large u_* and small w_*, and at small u_* and large w_*, as the relation that Hicks (1985) suggested:

$$\sigma_v^2 = 3.6u_*^2 + 0.35w_*^2. \tag{16}$$

Equations (14), (15), and (16) also evoke comparisons with gustiness parameterizations that are proving useful for estimating the turbulent surface fluxes over the ocean with bulk aerodynamic formulas, especially in light winds (e.g., Godfrey and Beljaars 1991; Fairall et al. 1996). Finally, written as (14), σ_h does not depend explicitly on z_i, which is the opposite conclusion that we would draw from (12).

4. Conclusions

Perhaps it is time to acknowledge that the horizontal velocity variances σ_u^2, σ_v^2, and σ_h^2 violate too many of the assumptions on which Monin–Obukhov similarity relies and to stop trying to force them into artificial similarity relations. In all but, maybe, the strongest winds, large eddies dictate the behavior of these variances. But these eddies reflect mesoscale variations in clouds, vegetation, surface slope, soil moisture, and the height of the boundary layer, among other parameters, and therefore cannot be in equilibrium with the local surface. Consequently, the largest eddies almost always violate the assumption of horizontal homogeneity that Monin–Obukhov similarity requires.

Acknowledgments. The U.S. Department of the Army supported ELA in this work through Project 4A161102AT24.

REFERENCES

Fairall, C. W., E. F. Bradley, D. P. Rogers, J. B. Edson, and G. S. Young, 1996: Bulk parameterization of air–sea fluxes for Tropical Ocean–Global Atmosphere Coupled-Ocean Atmosphere Response Experiment. *J. Geophys. Res.,* **101,** 3747–3764.

Godfrey, J. S., and A. C. M. Beljaars, 1991: On the turbulent fluxes of buoyancy, heat and moisture at the air–sea interface at low wind speeds. *J. Geophys. Res.,* **96,** 22 043–22 048.

Hicks, B. B., 1978a: Comments on 'The characteristics of turbulent velocity components in the surface layer under convective conditions,' by H. A. Panofsky, H. Tennekes, D. H. Lenschow, and J. C. Wyngaard. *Bound.-Layer Meteor.,* **15,** 255–258.

——, 1978b: Some limitations of dimensional analysis and power laws. *Bound.-Layer Meteor.,* **14,** 567–569.

——, 1981: An examination of turbulence statistics in the surface boundary layer. *Bound.-Layer Meteor.,* **21,** 389–402.

——, 1985: Behavior of turbulence statistics in the convective boundary layer. *J. Climate Appl. Meteor.,* **24,** 607–614.

——, 1995: Monin–Obukhov similarity—An historical perspective. Preprints, *11th Symp. on Boundary Layers and Turbulence,* Charlotte, NC, Amer. Meteor. Soc., 1–4.

Johansson, C., A.-S. Smedman, U. Högström, J. G. Brasseur, and S. Khanna, 2001: Critical test of the validity of Monin–Obukhov similarity during convective conditions. *J. Atmos. Sci.,* **58,** 1549–1566.

Kenney, B. C., 1982: Beware of spurious self-correlations. *Water Resour. Res.,* **18,** 1041–1048.

Panofsky, H. A., H. Tennekes, D. H. Lenschow, and J. C. Wyngaard, 1977: The characteristics of turbulent velocity components in the surface layer under convective conditions. *Bound.-Layer Meteor.,* **11,** 355–361.